



ELSEVIER

Contents lists available at ScienceDirect

## Advances in Colloid and Interface Science

journal homepage: [www.elsevier.com/locate/cis](http://www.elsevier.com/locate/cis)

Historical perspective

## Surface tension- and buoyancy-driven flows across horizontally propagating chemical fronts



R. Tiani\*, A. De Wit, L. Rongy

Nonlinear Physical Chemistry Unit, Faculté des Sciences, Université libre de Bruxelles (ULB), CP231, Brussels 1050, Belgium

## ARTICLE INFO

Available online 20 July 2017

## Keywords:

Surface tension-driven flows  
 Marangoni convection  
 Buoyancy-driven flows  
 Chemical fronts  
 Reaction-diffusion-convection systems

## ABSTRACT

Chemical reactions can interplay with hydrodynamic flows to generate various complex phenomena. Because of their relevance in many research areas, chemically-induced hydrodynamic flows have attracted increasing attention in the last decades. In this context, we propose to give a review of the past and recent theoretical and experimental works which have considered the interaction of such flows with chemical fronts, i.e. reactive interfaces, formed between miscible solutions. We focus in particular on the influence of surface tension- (Marangoni) and buoyancy-driven flows on the dynamics of chemical fronts propagating horizontally in the gravity field.

© 2017 Elsevier B.V. All rights reserved.

## Contents

1. Introduction	76
2. Surface tension- and buoyancy-driven flows traveling with autocatalytic chemical fronts	77
2.1. Autocatalysis and autocatalytic chemical fronts	77
2.2. Experimental studies	77
2.3. Theoretical studies	78
3. Surface tension- and buoyancy-driven flows traveling with bimolecular chemical fronts	79
3.1. Bimolecular chemical fronts	79
3.2. Experimental studies	80
3.3. Theoretical studies	80
4. Conclusive remarks and outlook	81
Acknowledgments	82
References	82

## 1. Introduction

By inducing compositional changes and possible thermal changes of the reactive medium, chemical reactions are likely to modify the physical properties of the solution (density, viscosity, surface tension) which may trigger convection. In that case, the evolution of the system is determined by the interaction between chemical and transport processes, specifically, diffusion and convective motions of the fluid. Such reaction-diffusion-convection (RDC) systems are not only relevant to engineering type processes but also to natural phenomena and environmental issues including air and water pollution, carbon sequestration and climate change. Complex

spatio-temporal dynamics of such systems may lead to the formation of spatial patterns of amazing beauty as well as to new hydrodynamic instabilities.

In this review, we will focus on chemical fronts which are a particular class of reactive systems. Such fronts are reactive interfaces resulting from the interplay between chemical reactions and diffusion. In systems closed to the air in which those fronts travel vertically, i.e. parallel to the gravity field, convective flows can typically be induced by density differences. The vast and rich literature devoted to the study of the resulting hydrodynamic instabilities will not be discussed here [1–4].

When the front propagates horizontally, i.e. perpendicularly to the gravity field, in systems open to the air, an additional source of convection arises due to possible surface tension gradients. The presence of both Marangoni (surface tension-driven) and buoyancy

\* Corresponding author.  
 E-mail address: [rtiani@ulb.ac.be](mailto:rtiani@ulb.ac.be) (R. Tiani).

(density-driven) effects then results in complex dynamics as will be described in this review.

Buoyancy-driven flows can easily be isolated if the experiment is undertaken in closed systems entirely filled with the reacting solutions for which no interface with air exists. On the other hand, it is more difficult to isolate the effect of Marangoni flows experimentally unless the experiments are carried out under microgravity conditions. Numerous experimental and theoretical works have studied those chemically-driven flows. We propose here to give an overview of the past and recent developments by giving particular attention to the influence of surface tension- and buoyancy-driven flows on the propagation of chemical fronts. In this review, we will not consider the case of immiscible systems for which Marangoni flows can also be observed at liquid/liquid interfaces [3,5–7]. We will therefore restrict our analysis to miscible reactive solutions, that can easily be classified depending on the type of chemical reactions considered: autocatalytic reactions [8–64] or bimolecular reactions [65–78].

We note that recent and detailed reviews of the literature already exist for the particular case of convective motions emerging when the autocatalytic Belousov-Zhabotinsky reaction takes place in thin solution layers [62] and droplets [63]. We therefore refer the interested readers to those review papers for a comprehensive overview into this complex and rich area.

Section 2 of this review will describe systems involving autocatalytic reactions while Section 3 will describe the case of bimolecular reactions producing a third species of the type  $A + B \rightarrow C$ . The conclusions and outlook will be drawn in the last section.

## 2. Surface tension- and buoyancy-driven flows traveling with autocatalytic chemical fronts

### 2.1. Autocatalysis and autocatalytic chemical fronts

Autocatalysis is a kinetic process involving feedback loops through which a reaction product catalyzes its own production. When autocatalysis is coupled to diffusion, it can lead to the formation of self-organized interfaces also called autocatalytic chemical fronts.

The properties of such fronts, studied experimentally in gels to prevent any convection, are well characterized and described by reaction-diffusion (RD) models [12,32,35]. In aqueous solutions, however, those fronts exhibit new dynamics that cannot be explained solely on the basis of RD equations. We first review the state of the art concerning the experimental works that have demonstrated, in particular, such new behaviors and discrepancies with respect to the RD theories. Finally, we introduce the theoretical works supporting these experiments or used to predict new spatio-temporal dynamics.

### 2.2. Experimental studies

Although wave fronts of the autocatalytic iodate-arsenous acid (IAA) reaction propagate at constant speed (and with a constant width) in gels where no convective motion is induced, they can undergo an acceleration in thin layers of solution in contact with air [8,9]. Similarly, the velocity of front propagation in the nitric acid-iron(II) reaction system can increase with time and depends on the depth of the solution layers in Petri dishes open to the air [13]. Those pioneering works were rapidly followed and similar results were obtained in the chlorite-thiosulfate reaction system [14]. Those experiments clearly demonstrate that convection plays an important role on the dynamics of fronts traveling in solution. Since inhomogeneities in the concentrations of species and in the temperature of the solution may arise when the front propagates, it was proposed

that a combination of both Marangoni and buoyancy-driven flows is at the origin of the observed convective motions in Petri dishes [16].

Such a combination was also shown to deeply affect the  $\text{BaSO}_4$ -precipitation patterns behind the traveling wave generated in the chlorite-thiourea-barium chloride reaction system [19,20,26,30,31,34] and to lead to the formation of thermal plumes in the same system [27].

Later, horizontally propagating fronts of the IAA reaction were studied in quasi-2D Hele-Shaw cells with no interface with air, thereby excluding Marangoni effects. Those fronts are deformed and their propagation speed is increased due to buoyancy-driven convection [48,51], which had already been observed in cylindrical tubes by Pojman et al. [17]. Results obtained for various heights of the liquid layer, stoichiometry (or chemical composition) and temperature, further revealed that a universal scaling exponent exists for the mixing length, defined as the standard deviation of the front position in the direction of propagation, with the height of the liquid layer when it is in the range of the centimeter. As long as the reaction front is sharp and no significant heat effects are present, the exponent is shown to be independent of chemical composition [51]. Similar results were obtained with the CT reaction [46].

By using 3D reactors open to the air, Šebestíková and Hauser observed additional phenomena such as the formation of multiple convection cells traveling with the IAA chemical waves [53]. Furthermore, the shape of the front across the width depends on the geometry and the resulting 3D convective flow fields. With the same reaction, Pópity-Tóth et al. showed that the contribution of Marangoni flows is greatly enhanced in sufficiently thin solution layers with an open surface [58,59]. The entire tilted reaction front becomes then 50% more elongated in the presence of Marangoni flows acting in the same direction as buoyancy-driven flows. The product solution of the IAA reaction has indeed both a lower density and a lower surface tension than the reactant solution. 3D simulations were also performed to support the experimental findings [59].

In contrast to the IAA reaction, the CT reaction is strongly exothermic. When it is operated under isothermal conditions, the product solution of the CT reaction is denser than the reactant one. Combined experimental and theoretical studies of chlorite-tetrathionate (CT) reaction fronts were undertaken in thin solution layers closed to the air (no Marangoni effects) [45,61]. The reported dynamics results from a competition between solutal and thermal effects leading in particular to oscillating flows [45]. We note that the addition of a macromolecule which binds the autocatalyst of the CT reaction, can not only decrease the velocity of front propagation but also lead to the formation of unusual cellular fingers [49,50]. Double-diffusive convection is shown to be among the driving forces in the pattern formation. In the same reactive system, Pópity-Tóth et al. have also studied how buoyancy effects affect the spatiotemporal pattern formation at various solution thicknesses [54]. A stationary structure propagating horizontally with constant velocity and geometry is found if the medium solution layer is sufficiently thick.

While the experiments presented above have all been performed in laboratories on earth, the propagation of IAA autocatalytic chemical fronts has been analyzed recently by Horváth et al. [60] during parabolic flights in which the gravity field is modulated periodically. By comparing measurements in uncovered and covered liquid layers, they could discriminate between surface tension- and density-driven flows and show their relative influence on the propagation and shape of the autocatalytic fronts. They found that the velocity and deformation of the front are increased during hyper-gravity phases and reduced in the micro-gravity phase. This is respectively due to the amplification or decay of the buoyancy-driven convective roll induced around the front while pure Marangoni-driven convection is not affected by the modulated gravitational field.

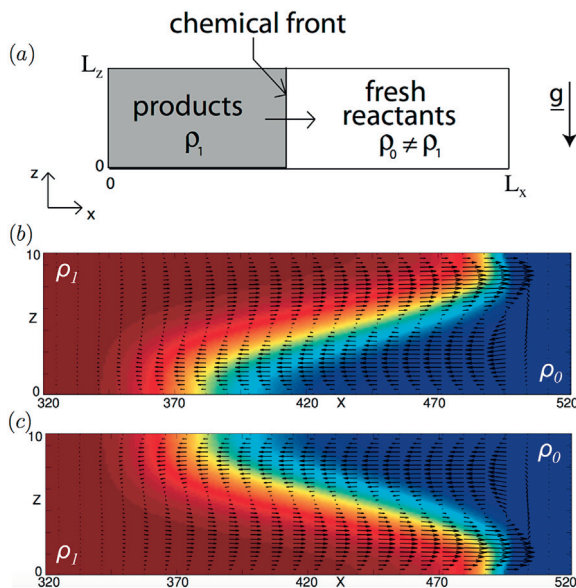


**Fig. 1.** Buoyancy-driven flows across an isothermal  $A + 2C \rightarrow 3C$  autocatalytic front in a covered thin solution layer. (a) Schematic of the system (not drawn to scale). The propagation of the front is initiated by a local addition of the autocatalytic species (the product). The product solution has a density  $\rho_1$  and propagates into the reactant solution of density  $\rho_0$ . We focus on the asymptotic convection roll traveling with the deformed front at a given time for (b)  $Ra = 100$  for which the less dense product solution in red invades the denser reactant solution in blue and (c)  $Ra = -100$  corresponding to the denser product solution invading the less dense reactant solution. The  $z$ -direction has been magnified in order to see the details of the velocity field [41].

The experiments mentioned here can be enlightened by the analysis of theoretical models as will be presented in the next section.

### 2.3. Theoretical studies

From a theoretical point of view, models typically include the RDC equations describing the evolution of the chemical concentrations and sometimes of temperature in the solution coupled to the incompressible Navier-Stokes equations used to model the fluid velocity field. These equations are solved using appropriated initial and boundary conditions which depend on the system considered. The experimental findings discussed above are well corroborated by these theoretical models.

Numerous studies have considered pure buoyancy-driven flows traveling with autocatalytic fronts in horizontal thin solution layers, evidencing the deformation of traveling pulses in excitable systems [18,24,25,28,33]. Vasquez et al. [21] and Jarrige et al. [47] have numerically shown that autocatalytic chemical fronts propagating horizontally in non-excitable systems can be accelerated and deformed by the presence of the convective flows developing across such fronts. Their predicted RDC speed for the IAA fronts is in good agreement with the values measured experimentally in thin horizontal tubes.

Rongy et al. quantitatively studied how those buoyancy-driven flows affect an isothermal autocatalytic front of the type  $A + 2C \rightarrow 3C$  in covered horizontal thin solution layers (Fig. 1) [41]. The density of the product solution  $\rho_1$  differs from that of the reactant solution  $\rho_0$  since these two states correspond to different concentrations (Fig. 1 (a)). The resulting horizontal density differences across the front induce convective motions in the solution which in turn affect the initially vertical RD front as well as its dynamics. In this case, the

coupling between RD processes and buoyancy-driven convection is quantified by the solutal Rayleigh number  $Ra$  defined as

$$Ra = -\frac{d\rho}{dc} \frac{a_0 L_c^3 g}{D\mu}, \quad (1)$$

where  $\rho$  is the solution density,  $\mu$  the dynamic viscosity,  $c$  the product concentration,  $a_0$  the initial concentration of reactant solution,  $D$  the molecular diffusion coefficient of the product,  $g = |g|$  is the gravity acceleration,  $L_c$  the characteristic length scale of the RD system, i.e.  $L_c = \sqrt{D/(ka_0^2)}$  where  $k$  is the rate constant of the autocatalytic reaction. When the Rayleigh number  $Ra$  is positive, the density decreases during the reaction meaning that the product solution behind the front is less dense than the reactant solution and naturally rises above it when the front travels horizontally in the gravity field (Fig. 1 (b)). On the contrary, when  $Ra < 0$ , the density increases during the reaction and the denser product solution sinks below the less dense reactant solution (Fig. 1 (c)). The system reaches an asymptotic dynamic state characterized by a deformed front and a steady localized convection roll, both traveling at the same constant speed, larger than the speed of the RD planar front. A parametric study shows that the intensity of the flow, the propagation speed, and the deformation of the front are increasing functions of the absolute value of the Rayleigh number  $|Ra|$  and of the layer thickness  $L_z$ .

The influence of thermal effects on the system dynamics depends on two parameters, a Lewis number  $Le$  and a thermal Rayleigh number  $R_T$  defined, respectively, as

$$Le = D_T/D, \quad (2)$$

$$R_T = -\frac{d\rho}{dT} \frac{\Delta T L_c^3 g}{D\mu}, \quad (3)$$

with the thermal diffusivity  $D_T = \kappa_T/(\rho_0 c_p)$  where  $c_p$  is the specific heat capacity of the solution,  $\kappa_T$  its thermal conductivity.  $\Delta T$  represents the adiabatic temperature rise in the reaction zone with  $\Delta T = -\Delta H a_0/(\rho_0 c_p)$  being positive since the reaction enthalpy  $\Delta H$  is assumed to be negative corresponding to exothermic reactions. No endothermic autocatalytic reactions are known up to now [44].

Two different types of systems can be distinguished: cooperative systems where solutal and thermal effects both contribute to a

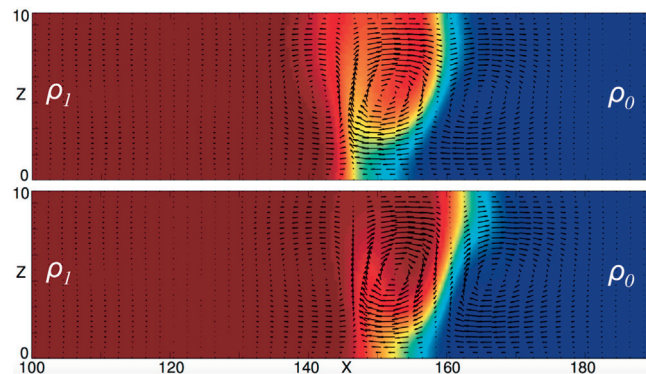


**Fig. 2.** Buoyancy-driven flows across an exothermic  $A + 2C \rightarrow 3C$  autocatalytic front in a covered thin solution layer. Focus on the oscillating fluid velocity field traveling at a constant speed with the concentration front for  $Ra = -10$ ,  $R_T = 15$  and  $Le = 5$ . The figures are shown at  $t = 42, 45$ , top to bottom. The hot but denser product solution, are shown in red invading the cold but lighter reactant solution, shown in blue. The  $z$ -direction has been magnified in order to see the details of the velocity field [44].

decrease of the solution density during the reaction and antagonist systems when the solutal contribution corresponds to an increase of the solution density during the reaction whereas the products are hotter. In the cooperative case, typically corresponding to the IAA reaction, the system always reaches an asymptotic dynamics, with the exothermic front featuring a permanent deformed shape similar to the one encountered in the isothermal situation. On the other hand, antagonistic effects are observed to lead to an oscillatory dynamics in a frame still propagating at a constant speed when the overall density of the product solution is sufficiently smaller than that of the reactant solution (Fig. 2). Similar behaviors called “rolling chemical wave” were observed in experiments with the autocatalytic chlorite–thiosulfate reaction [14] and with the CT reaction [45], both reactions for which solutal and thermal effects are competing.

Similarly to the buoyancy-driven case, the propagation of autocatalytic chemical fronts has been studied when only capillary flows are present in thin layers of solution in contact with air [37]. In this case, the reaction which takes place in the bulk produces a surface-active species so that the surface tension of the products  $\gamma_1$  differs from that of the reactants  $\gamma_0$  (Fig. 3 (a)). Therefore, the governing equations for this system are obtained by coupling the RDC equation for the surface-active product concentration to the incompressible Navier-Stokes equations describing the flow field evolution. A specific Marangoni boundary condition is used for the horizontal fluid velocity at the surface. No surface deformation (i.e. the capillary number is small so that surface tension dominates over pressure and normal viscous stress effects) and no evaporation, are assumed so that the air layer is not considered in that work.

The system reaches a steady regime too, characterized by a convection roll traveling with the chemical front at a constant speed. In that system, the intensity of the coupling between RD processes and convection is quantified by a solutal Marangoni number  $M$  defined as

$$M = -\frac{1}{\mu\sqrt{Dk}} \frac{d\gamma}{dc}, \quad (4)$$

where  $\gamma$  is the solution surface tension and  $c$  the concentration of the surface-active product. As can be observed in Fig. 3 (b), for positive Marangoni numbers, the product of the reaction decreases the surface tension behind the front leading to a clockwise convective roll ( $\gamma_0 > \gamma_1$ ) while for negative Marangoni numbers (Fig. 3 (c)), the product increases the surface tension behind the front and a counterclockwise convective roll is observed ( $\gamma_0 < \gamma_1$ ). The front deformation, its constant propagation speed, and the convective motions all increase with the absolute value of the solutal Marangoni number  $|M|$  and with the layer thickness  $L_z$ . However, an important difference between buoyancy- and Marangoni-driven convection traveling with such fronts is the behavior for negative  $Ra$  and  $M$ . Indeed the situation at negative Rayleigh numbers can be obtained by symmetry with respect to the positive  $Ra$  case while there is an asymmetry between the results obtained for positive and negative Marangoni numbers. The different characteristics of the dynamics between  $M > 0$  and  $M < 0$  can be explained by the fact that Marangoni flows are driven and sustained by forces at the surface [43]. Similar results have recently been obtained by Guzman et al. where the IAA front propagation is modeled, in the approximation of a thin front, by the deterministic Kardar–Parisi–Zhang equation modified to account for the fluid flow [64].

To take into account the exothermicity of the autocatalytic reactions, an additional RDC equation for the evolution of the temperature can be added [56]. An additional thermal Marangoni number is then introduced to measure the effect of temperature on the surface tension. When both solutal and thermal effects act as to decrease the surface tension during the reaction, the dynamics is referred to as cooperative and the system attains an

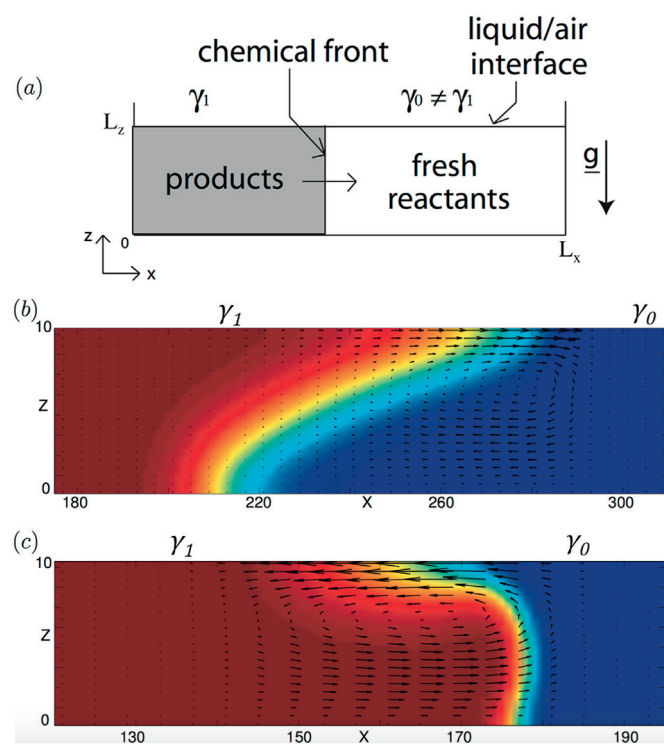


**Fig. 3.** Surface tension-driven flows across an isothermal  $A + 2C \rightarrow 3C$  autocatalytic front in a thin solution layer open to the air. (a) Sketch of the system (not drawn to scale). Due to the surface tension changes at the liquid/air interface, solutal Marangoni flows are induced across the chemical front. We focus on the asymptotic Marangoni-driven convective roll traveling with the deformed front at a given time for (b)  $M = 100$  and (c)  $M = -100$  with the products in red invading the reactants shown in blue. The  $z$ -direction has been magnified in order to see the details of the velocity field [37].

asymptotic regime similar to the isothermal situation. In the case of antagonistic effects, the difference in diffusivities of heat and mass can lead to an oscillatory dynamics characterized by oscillations of the concentration, temperature and velocity fields. The combination of both Marangoni and buoyancy-driven flows induced around chemical fronts has been shown to induce oscillations of the fronts as well, even in the isothermal case where no differential diffusivities effects are at play [57].

Finally, we note that the interaction between surface-tension driven flows and bistable reactions has also been the subject of many interesting theoretical studies which mainly focus on thin films [10,11,15,29,38–40,42,52].

### 3. Surface tension- and buoyancy-driven flows traveling with bimolecular chemical fronts

#### 3.1. Bimolecular chemical fronts

Second-order chemical reactions of the form  $A + B \rightarrow C$  can also sustain a reaction-diffusion front, as soon as the reactants are initially separated in space [65]. The dynamics of this front can be described by several quantities such as the local production rate  $R = kab$  with  $k$  the kinetic constant of the chemical reaction, the location of the reaction front  $x_f$  defined as the position along  $x$  where the production rate reaches its maximum value, or the width of the reaction zone  $w$ , defined as the square root of the second moment of the production rate distribution.

We note that a bimolecular front is fundamentally different from an autocatalytic front. Indeed, as stated in the previous section, the

latter is a self-sustained interface separating the products and the reactants of an autocatalytic reaction and travels in gels with a constant width and speed. On the other hand, a bimolecular front results from the particular initial condition of segregated reactants and travels in gels with a width increasing in time and, in general, at a non-constant diffusive speed.

It is already well-known that without convection, if the reactants are initially equally concentrated and diffuse at the same rate, the diffusive fluxes of reactants A and B towards the reaction zone are identical, and the position of the bimolecular reaction front therefore remains at its initial position ( $x_f = 0$ ) [65]. Otherwise, such a front moves in time towards the side with the smallest diffusive flux ( $x_f \neq 0$ ) [67,68].

While the results reported above have been performed under the assumption that the system is infinite in either direction, the geometrical properties of the reaction front have also been investigated when an imposed flux  $j$  of A and B species is injected at opposite extremities of a finite domain [69]. The front properties are then shown to depend on  $j$ . In particular, in the steady state, the reaction zone width is proportional to  $j^{-1/3}$  in the large flux limit, and the concentration of each species within this zone is of order  $j^{2/3}$ . On the opposite case, in the limit of small flux, the concentration takes a nearly constant value throughout the system and is proportional to  $j^{1/2}$  [69].

Finally, we note that fluctuation effects observed due to the confinement of the reaction front in one dimension have also been widely studied both with no-fluxes [70] and imposed fluxes [71] boundary conditions but always in the absence of convection.

Numerous experimental and theoretical works have been performed to extend such results in the presence of convective motions. We propose to summarize them below, even though it has to be pointed out that fewer studies are available in the literature compared to the case of autocatalytic chemical fronts.

### 3.2. Experimental studies

Similarly to the case of autocatalytic fronts, the RD properties of  $A + B \rightarrow C$  fronts are nowadays well understood and validated by experiments performed in gels, such as the complexation of copper studied by Koo and Kopelman [66]. However, Park et al. studied the same reaction in the absence of a gel, in a solution contained between two horizontal microscope slides separated by a narrow gap [74]. They found that the front position scales with time as  $t^\alpha$  where  $\alpha = 0.60$  is larger than the exponent  $\alpha = 1/2$  predicted in the pure RD case. Similar discrepancies for the scaling exponent of the front position with time were obtained by Shi and Eckert in their experimental study of a neutralization reaction front in a horizontal Hele-Shaw cell [5]. Moreover, in the latter case, the front is also shown to be accelerated by at least a factor of four compared with the RD case. Thus, in the absence of a gel, the experimental front moves faster than expected by the RD theories [6,65] which is more than likely to be due to the presence of chemically-driven hydrodynamic flows.

More recently, Eckert et al. performed microgravity experiments in horizontal closed Hele-Shaw cells considering an acid (A = propionic acid) and a base (B = TMAH) as reactants to give a salt (C = tetramethylammonium propionate) [77]. They showed that gravity strongly affects the motion of such bimolecular fronts, even in thin fluid layers, due to the amplification or decay of a buoyancy-driven double vortex surrounding the front when increasing or decreasing the gravity level.

### 3.3. Theoretical studies

By solving numerically the incompressible Stokes equations coupled to the RDC equations governing the evolution of the

concentrations of A, B and C, Rongy et al. provided the first theoretical study of the influence of pure buoyancy-driven flows on the motion of isothermal  $A + B \rightarrow C$  reaction fronts for equal initial concentrations of reactants and diffusion coefficients of all species [75].

Since the problem involves now three chemical species, three solutal Rayleigh numbers  $R_{a,b,c}$  are required to quantify the influence of each chemical species concentration on the solution density, that we define as

$$R_i = \frac{d\rho}{dc_i} \frac{a_0 g L_c^3}{\mu D}, \quad (5)$$

where  $c_i$  is the concentration of the corresponding species,  $D$  the diffusion coefficient supposed to be the same for all species and  $L_c$  the characteristic length of the corresponding RD system noted  $L_c = \sqrt{D/(ka_0)}$ . Furthermore, the solutes are all supposed to increase the density of water, such that only positive values for  $R_{a,b,c}$  have been considered.

Fig. 4 (a) shows the initial configuration of the system where the reactants are brought into contact at  $x = 0$  and react to produce a reaction front. In the course of time, the product C is formed in the reaction zone and diffuses towards the reactants. Since the three chemical species can affect the density of the solution, buoyancy flows are induced across the front. The length of the system  $L_x$  is chosen sufficiently large so that the results are not affected by boundary effects on the time of interest, typically  $L_x = 300$ .

In Fig. 4 (b), density plots of the concentrations  $a, b, c$ , and (dimensionless) production rate  $ab$  are illustrated for the case where species C is the most dense and so sinks to the bottom, while the less

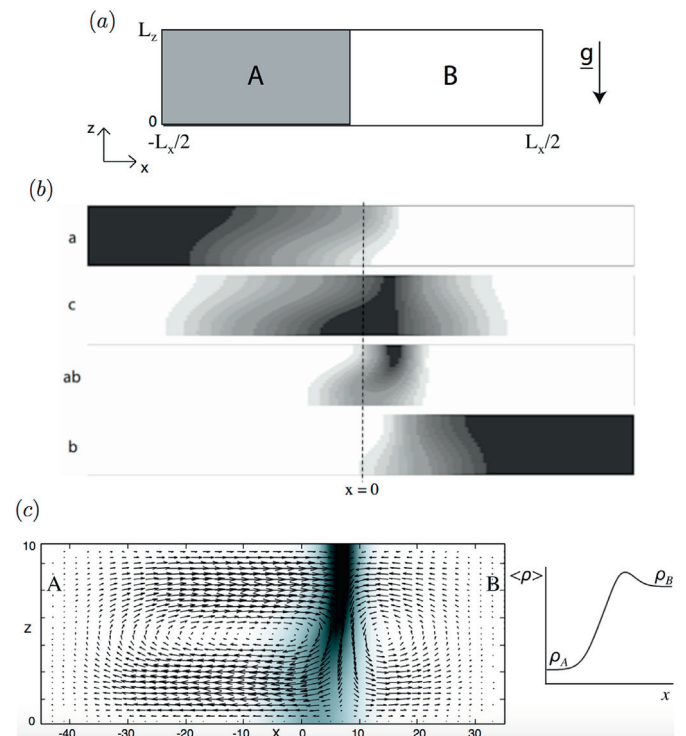


**Fig. 4.** Buoyancy-driven flows around an isothermal  $A + B \rightarrow C$  reaction front in a covered thin solution layer. (a) Sketch of the system (not drawn to scale). (b) Density plots of  $a, c, ab$  (dimensionless production rate), and  $b$ , centered on the reaction zone for the Rayleigh numbers  $R_a = 2, R_b = 4$ , and  $R_c = 10$ , when the density of C is the largest. (c) Focus on the convection rolls traveling with the deformed reaction front (or  $ab$ ) for the same Rayleigh numbers. The typical density profile corresponding to the observed convective rolls is also drawn, varying between  $\rho_A$  (the solution density of A) and  $\rho_B$  (the solution density of B). The layer is shown at time  $t = 50$ . Dark regions correspond to high concentrations/production rate with the maximum in black and the minimum in white [75].

dense A and B rise to the top. This generates a convective roll turning clockwise on the left where C sinks below A and a second counter-clockwise convective roll on the right where C sinks below B (Fig. 4 (c), left). The typical depth-averaged density profile corresponding to the observed convective rolls is also drawn at the right-hand side of Fig. 4 (c). The solution density varies between  $\rho_A$  (the solution density of A) and  $\rho_B$  (the solution density of B) and reaches its maximum value in the reaction zone (the region between A and B solutions where C is produced). Because the variation of density is larger on the left side of the maximum, a strongest convective roll is observed on this side. This asymmetry yields a global acceleration of the front to the right as can be seen in Fig. 4 (c). Convective motions can therefore lead to front propagation even in the case of equal diffusion coefficients and initial concentrations of reactants for which RD scalings predict a nonmoving front.

Based on the pure RD equations, all possible density profiles and related flow properties can be classified in a parameter space spanned by the Rayleigh numbers of the problem [75]. Those theoretical predictions have later been supported by the experimental results obtained by Eckert et al. in modulated gravity [77].

In the case where the reactants have different initial concentrations, the system can exhibit a reversal in the direction of propagation of the reaction front [76]. Such a front reversal exists because diffusion and buoyancy convection can act in the opposite direction for some values of the Rayleigh numbers  $R_{a,b,c}$ . This change in the direction of the front is observed even for equal diffusion coefficients of the reactants. This is thus a peculiar feature of the RDC system. Indeed, it is also possible to observe such a front dynamics in the absence of convection but only for different diffusion coefficients and initial concentrations of the reactants [72,73].

In the same spirit, Tiani and Rongy have studied the influence of pure Marangoni flows induced across such fronts for equal initial concentrations of reactants and diffusion coefficients of all species assuming the solution density as constant [78]. The liquid/air interface is taken into account and each chemical species can affect the solution surface tension. The sketch of the system is then basically the same as in Fig. 4 (a) but now the fluid layer is open to the air.

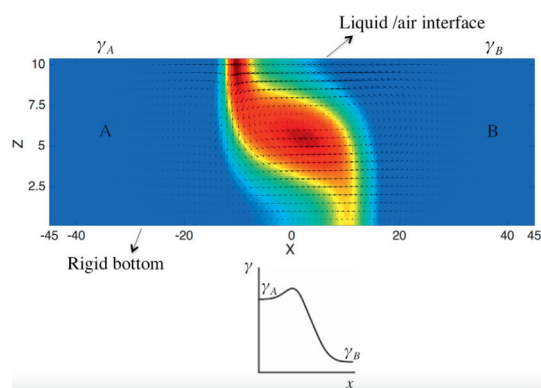


**Fig. 5.** Surface tension-driven flows around an isothermal  $A + B \rightarrow C$  reaction front in a thin solution layer open to the air. Focus on the convective rolls centered on the deformed reaction front (or production rate) shown for  $M_a = 20$ ,  $M_b = 40$  and  $M_c = 25$  and at time  $t = 30$ . The fluid velocity field is superimposed on a 2D plot of the production rate which ranges between its maximum value shown in red, and its minimum value shown in blue. The typical surface tension profile corresponding to the observed convective rolls is also drawn just below. The solution surface tension varies between  $\gamma_A$  (the surface tension of solution A) and  $\gamma_B$  (the surface tension of solution B) and reaches its maximum value in the reaction zone. Because the variation of surface tension is larger on the right side of the maximum, a strongest convective roll is observed on this side. The  $z$ -direction has been magnified to see the details of the velocity field [78].

The governing equations in this layer are therefore obtained by coupling the RDC equations to the incompressible Navier-Stokes equations, subject to a Marangoni boundary condition for the horizontal component of the fluid flow at the surface ( $z = L_z$ , where  $L_z$  is the layer thickness) to include surface tension effects. The main assumptions are no surface deformation, no evaporation processes and no released heat during the chemical reaction (isothermal reaction). In this case, the front dynamics is governed by the solutal Marangoni numbers of species A, B and C which quantify the influence of each chemical species on the solution surface tension and are defined as

$$M_i = -\frac{1}{\mu} \frac{\partial \gamma}{\partial c_i} \sqrt{\frac{a_0}{Dk}} \quad (6)$$

Each chemical species is supposed to decrease the surface tension of water, which is more likely to be the case experimentally, corresponding thus to positive values for the solutal Marangoni numbers  $M_{a,b,c}$ .

The resulting structure of Marangoni flows propagating with the reaction front is illustrated when the surface tension in the reaction zone is larger than the surface tension of A and B solutions (Fig. 5). This leads to the formation of two convective rolls in the solution while the strongest one is observed on the right side because the variation of the surface tension is largest on this side as seen in the corresponding schematic surface tension profile (Fig. 5, down).

More surprisingly, due to the structure of Marangoni flows, it has been shown that these flows lead to more complex and exotic properties of the front compared to density-driven flows. This can intuitively be explained as follows. In the case of closed systems where only buoyancy-driven flows are observed, the identical no-slip boundary conditions at the surface and the bottom allow the flows to possess a symmetry around the horizontal axis  $z = L_z/2$  (Fig. 4 (c), left). However, in the presence of an open surface and Marangoni flows, such a symmetry is lost affecting deeply the front properties. A simple consequence of this asymmetry can be seen in Fig. 5 (top) where a strong deformation of the front is observed for short times due to the action of the return flow (of the strongest convective roll) which extends from the bottom ( $z = 0$ ) to about two-third of the height ( $z \simeq 2L_z/3$ ).

Therefore, the main difference between buoyancy-driven and Marangoni flows arises from the change of boundary conditions for the fluid velocity field between the two cases. The resulting asymmetric Marangoni flows deeply alter the front propagation, even possibly reversing its direction in the course of time for some values of the Marangoni numbers. This unexpected front reversal is therefore of a completely different nature than the one described above for buoyancy-driven flows, when different initial concentrations of reactants are chosen.

A new classification of the convective dynamics of  $A + B \rightarrow C$  reaction fronts has finally been proposed as a function of the Marangoni numbers of the three chemical species [78].

#### 4. Conclusive remarks and outlook

The interaction between chemical reactions, diffusion and convection usually leads to complex and fascinating spatio-temporal dynamics and is encountered in various research areas such as sequestering carbon dioxide, modeling of industrial reactive flows or understanding complexity in nature, to name but a few. We have reviewed here the past and recent experimental and theoretical studies which have considered horizontally oriented set-up (typically Petri dishes or horizontal Hele-Shaw cells) in which chemical reactions coupled to diffusion give rise to concentration and/or temperature gradients inducing themselves density or surface tension

gradients in solution. Such reaction-diffusion-convection (RDC) systems have typically been studied for two classes of chemical fronts: autocatalytic fronts converting the reactants into the products and bimolecular  $A + B \rightarrow C$  type reaction fronts. Both types of fronts have been analyzed when traveling perpendicularly to the gravity field in solution layers, in the presence of buoyancy-driven and/or Marangoni flows. We have furthermore provided in this review some of the results inspired from our models to show typically what can be observed in those conditions.

From a chemical point of view, all these works have shown that the presence of convection, independently of its nature, drastically affects the properties of reaction-diffusion (RD) systems since the front is deformed across the layer and travels faster than in the absence of convection. The chemical dynamics of the system is therefore deeply altered by convective motions. From a hydrodynamic point of view, those studies also present a great interest because the source of the localized reactive flows considered here are internal to the RD dynamics which generates autonomous localized gradients of concentration (and temperature) in the solution across the front. This is in contrast with non-reactive flows which are usually either non-localized or arise from an externally applied local gradient in the fluid properties, for instance by heating the solution locally.

In the case of autocatalytic fronts propagating horizontally in the gravity field, a possible extension of those works would be to consider nonidealities in the governing equations, which would be typically relevant for concentrated solutions. The solution density or surface tension would then depend nonlinearly on the concentration of each chemical species, and corrections would have to be included in kinetic and transport terms.

In the case of  $A + B \rightarrow C$  reaction fronts traveling horizontally in the gravity field, fewer studies are reported and thus much more possible extensions could be considered with respect to the autocatalytic case. Since our analysis of the propagation of such fronts has been carried out in the case of equal diffusion coefficients of the chemical species for pure buoyancy-driven flows and pure Marangoni flows, a natural extension would be to consider the case of different diffusion coefficients. That study will not only be useful to complete the picture of the front dynamics but also to highlight the specificity of each type of flow on the front properties. A general model coupling Marangoni and buoyancy convection both arising from concentration and temperature gradients could next be examined. The effects of the reversibility of the chemical reaction, nonidealities in transport and kinetic terms or the study of the front propagation in thin films where Marangoni convection is expected to dominate with respect to buoyancy-driven flows could also be of great interest to investigate both theoretically and experimentally in future works.

In the light of the important applications of the works reported in this review, it is clear that multidisciplinary collaborative efforts of chemists, physicists, and engineers are needed to provide new insights into this emerging domain of nonlinear sciences.

## Acknowledgments

The authors thank the “Actions de Recherches Concertées” program, the F.R.S. - FNRS and Prodex for financial support.

## References

- [1] D'Hernoncourt J, Zebib A, De Wit A. On the classification of buoyancy-driven chemo-hydrodynamic instabilities of chemical fronts. *Chaos* 2007;17:013109.
- [2] De Wit A. Chemo-hydrodynamic patterns and instabilities. *Chim Nouv* 2008;99:1–7.
- [3] De Wit A, Eckert K, Kalliadasis S. Introduction to the focus issue: chemo-hydrodynamic patterns and instabilities. *Chaos* 2012;22:037101.
- [4] Lemaigre L, Budroni MA, Riolfi LA, Grosfils P, De Wit A. Asymmetric Rayleigh-Taylor and double-diffusive fingers in reactive systems. *Phys fluids* 2013;25:014103.
- [5] Shi Y, Eckert K. Acceleration of reaction fronts by hydrodynamic instabilities in immiscible systems. *Chem Eng Sci* 2006;61:5523–33.
- [6] Trevelyan PMJ, Strier DE, De Wit A. Analytical asymptotic solutions of  $nA + mB \rightarrow C$  reaction-diffusion equations in two-layer systems: a general study. *Phys Rev E* 2008;78:026122.
- [7] Schwarzenberger K, Köllner T, Linde H, Boeck T, Odenbach S, Eckert K. Pattern formation and mass transfer under stationary solutal Marangoni instability. *Adv Colloid Interf Sci* 2014;206:344–71.
- [8] Gribshaw TA, Showalter K, Banville DL, Epstein IR. Chemical waves in the acidic iodate oxidation of arsenite. *J Phys Chem* 1981;85:2152–5.
- [9] Hanna A, Saul A, Showalter K. Detailed studies of propagating fronts in the iodate oxidation of arsenous acid. *J Am Chem Soc* 1982;104:3838–44.
- [10] Dagan Z, Pismen LM. Marangoni waves induced by a multistable chemical reaction on thin liquid films. *J Colloid Interface Sci* 1984;99:215–25.
- [11] Pismen LM. Composition and flow patterns due to chemo-Marangoni instability in liquid films. *J Colloid Interf Sci* 1984;102:237–47.
- [12] Saul A, Showalter K. Propagating reaction-diffusion fronts. In: *RJ, Field M, Burger, eds. Oscillations and traveling waves in chemical systems.* New York: Wiley 1985. p. 419–39.
- [13] Bazsa G, Epstein IR. Traveling waves in the nitric acid-iron(II) reaction. *J Phys Chem* 1985;89:3050–3.
- [14] Nagypál I, Bazsa G, Epstein IR. Gravity-induced anisotropies in chemical waves. *J Am Chem Soc* 1986;108:3635–40.
- [15] Dagan Z, Maldarelli C. The influence of surface tension on propagating chemo-hydrodynamic waves. *Chem Eng Sci* 1987;42:1259–61.
- [16] Pojman JA, Epstein IR. Convective effects on chemical waves. 1. Mechanisms and stability criteria. *J Phys Chem* 1990;94:4966–72.
- [17] Pojman JA, Epstein IR, McManus TJ, Showalter K. Convective effects on chemical waves. 2. Simple convection in the iodate-arsenous acid system. *J Phys Chem* 1991;95:1299–306.
- [18] Plesser T, Wilke H, Winters KH. Interaction of chemical waves with convective flows induced by density gradients. a comparison between experiments and computer simulations. *Chem Phys Lett* 1992;200:158–62.
- [19] Hauser MJB, Simoyi RH. Inhomogeneous precipitation patterns in a chemical wave. *Phys Lett A* 1994;191:31–8.
- [20] Hauser MJB, Simoyi RH. Inhomogeneous precipitation patterns in a chemical wave. Effect of thermocapillary convection. *Chem Phys Lett* 1994;227:593–600.
- [21] Vasquez DA, Little JM, Wilder JW, Edwards BF. Convection in chemical waves. *Phys Rev E* 1994;50:280–4.
- [22] Nagy IP, Keresztessy A, Pojman JA, Bazsa G, Noszticzus Z. Chemical waves in the iodide-nitric acid system. *J Phys Chem* 1994;98:6030–7.
- [23] Keresztessy A, Nagy IP, Bazsa G, Pojman JA. Traveling waves in the iodate-sulfite and bromate-sulfite systems. *J Phys Chem* 1995;99:5379–84.
- [24] Wilke H. Interaction of traveling chemical waves with density driven hydrodynamic flows. *Physica D* 1995;86:508–13.
- [25] Wu Y, Vasquez DA, Edwards BF, Wilder JW. Convective chemical wave propagation in the Belousov-Zhabotinsky reaction. *Phys Rev E* 1995;51:1119–27.
- [26] Martincigh BS, Simoyi RH. Convective instabilities induced by an exothermic autocatalytic chemical reaction. *Phys Rev E* 1995;52:1606–13.
- [27] Martincigh BS, Hauser MJB, Simoyi RH. Formation of thermal plumes in an autocatalytic exothermic chemical reaction. *Phys Rev E* 1995;52:6146–53.
- [28] Matthiessen K, Wilke H, Müller SC. Influence of surface tension changes on hydrodynamic flow induced by traveling chemical waves. *Phys Rev E* 1996;53:6056–60.
- [29] Pismen LM. Interaction of reaction-diffusion fronts and Marangoni flow on the interface of a deep fluid. *Phys Rev Lett* 1997;78:382–5.
- [30] Chinake CR, Simoyi RH. Experimental studies of spatial patterns produced by diffusion-convection-reaction systems. *J Chem Soc Faraday Trans* 1997;93:1345–50.
- [31] Martincigh BS, Chinake CR, Howes T, Simoyi RH. Self-organization with traveling waves: a case for a convective torus. *Phys Rev E* 1997;55:7299–303.
- [32] Epstein IR, Pojman JA. An introduction to nonlinear chemical dynamics: oscillations, waves, patterns, and chaos. Oxford University Press: New York; 1998.
- [33] Pérez-Villar V, Muñuzuri AP, Pérez-Muñuzuri V. Convective structures in a two-layer gel-liquid excitable medium. *Phys Rev E* 2000;61:3771–6.
- [34] Martincigh BS, Simoyi RH. Pattern formation fueled by dissipation of chemical energy: conclusive evidence for the formation of a convective torus. *J Phys Chem A* 2002;106:482–9.
- [35] Van Saarloos W. Front propagation into unstable states. *Phys Report* 2003;386:29–222.
- [36] Sakurai T, Inomoto O, Miike H, Kai S. Structure of surface deformation waves induced in spiral pattern in the Belousov-Zhabotinsky reaction. *J Phys Soc Jpn* 2004;73:485–90.
- [37] Rongli L, De Wit A. Steady Marangoni flow traveling with chemical fronts. *J Chem Phys* 2006;124:164705.
- [38] Pereira A, Trevelyan PMJ, Thiele U, Kalliadasis S. Dynamics of a horizontal thin liquid film in the presence of reactive surfactants. *Phys Fluids* 2007;19:112102.
- [39] Pereira A, Trevelyan PMJ, Thiele U, Kalliadasis S. Interfacial hydrodynamic waves driven by chemical reactions. *J Eng Math* 2007;59:207–20.

- [40] Pereira A, Trevelyan PMJ, Thiele U, Kalliadasis S. Thin films in the presence of chemical reactions. *FDMP* 2007;3:303–16.
- [41] Rongy L, Goyal N, Meiburg E, De Wit A. Buoyancy-driven convection around chemical fronts traveling in covered horizontal solution layers. *J Chem Phys* 2007;127:114710.
- [42] Rongy L, De Wit A. Solitary Marangoni-driven convective structures in bistable chemical systems. *Phys Rev E* 2008;77:046310.
- [43] Rongy L, De Wit A, Homsy GM. Asymptotic structure of steady nonlinear reaction-diffusion-Marangoni convection fronts. *Phys Fluids* 2008;20:072103.
- [44] Rongy L, De Wit A. Buoyancy-driven convection around exothermic autocatalytic chemical fronts traveling horizontally in covered thin solution layers. *J Chem Phys* 2009;131:184701.
- [45] Rongy L, Schusztzer G, Sinkó Z, Tóth T, Horváth D, Tóth Á. et al. Influence of thermal effects on buoyancy-driven convection around autocatalytic chemical fronts propagating horizontally. *Chaos* 2009;19:023110.
- [46] Schusztzer G, Tóth T, Horváth D, Tóth Á. Convective instabilities in horizontally propagating vertical chemical fronts. *Phys Rev E* 2009;79:016216.
- [47] Jarrige N, Bou Malham I, Martin J, Rakotomalala N, Salin D, Talon L. Numerical simulations of a buoyant autocatalytic reaction front in tilted Hele-Shaw cells. *Phys Rev E* 2010;81:066311.
- [48] Bou Malham I, Jarrige N, Martin J, Rakotomalala N, Talon L, Salin D. Lock-exchange experiments with an autocatalytic reaction front. *J Chem Phys* 2010;133:244505.
- [49] Rica T, Pópity-Tóth E, Horváth D, Tóth Á. Double-diffusive cellular fingering in the horizontally propagating fronts of the chlorite-tetrathionate reaction. *Physica D* 2010;239:831–7.
- [50] Miholics O, Rica T, Horváth D, Tóth Á. Oscillatory and stationary convective patterns in a reaction driven gravity current. *J Chem Phys* 2011;135:204501.
- [51] Pópity-Tóth E, Horváth D, Tóth Á. The dependence of scaling law on stoichiometry for horizontally propagating vertical chemical fronts. *J Chem Phys* 2011;135:074506.
- [52] Pismen LM. Solitary structures sustained by Marangoni flow. *Math Model Nat Phenom* 2011;6:48–61.
- [53] Šebestíková L, Hauser MJB. Buoyancy-driven convection may switch between reactive states in three-dimensional chemical waves. *Phys Rev E* 2012;85:036303.
- [54] Pópity-Tóth E, Horváth D, Tóth Á. Horizontally propagating three-dimensional chemo-hydrodynamic patterns in the chlorite-tetrathionate reaction. *Chaos* 2012;22:037105.
- [55] Rossi F, Budroni MA, Marchettini N, Carballido-Landeira J. Segmented waves in a reaction-diffusion-convection system. *Chaos* 2012;22:037109.
- [56] Rongy L, Assemat P, De Wit A. Marangoni-driven convection around exothermic autocatalytic chemical fronts in free-surface solution layers. *Chaos* 2012;22:037106.
- [57] Budroni MA, Rongy L, De Wit A. Dynamics due to combined buoyancy- and Marangoni-driven convective flows around autocatalytic fronts. *Phys Chem Chem Phys* 2012;14:14619–29.
- [58] Pópity-Tóth E, Pimienta V, Horváth D, Tóth Á. Hydrodynamic instability in the open system of the iodate-arsenous acid reaction. *J Chem Phys* 2013;139:164707.
- [59] Pópity-Tóth E, Pótári G, Erdős I, Horváth D, Tóth Á. Marangoni instability in the iodate-arsenous acid reaction front. *J Chem Phys* 2014;141:044719.
- [60] Horváth D, Budroni MA, Bába P, Rongy L, De Wit A, Eckert K. et al. Convective dynamics of traveling autocatalytic fronts in a modulated gravity field. *Phys Chem Chem Phys* 2014;16:26279.
- [61] Schusztzer G, Pótári G, Horváth D, Tóth Á. Three-dimensional convection-driven fronts of the exothermic chlorite-tetrathionate reaction. *Chaos* 2015;25:064501.
- [62] Miike H, Sakurai T, Nomura A, Müller SC. Chemically driven convection in the Belousov-Zhabotinsky reaction - evolutionary pattern dynamics. *Forma* 2015;30:S33–S53.
- [63] Miyazaki S, Sakurai T, Kitahata H. Coupling between a chemical wave and motion in a Belousov-Zhabotinsky droplet. *Current Phys Chem* 2015;5:82–90.
- [64] Guzman R, Vasquez DA. Surface tension driven flow on a thin reaction front. *Eur Phys J Special Topics* 2016;225:2573–80.
- [65] Gálfi L, Rácz Z. Properties of the reaction front in an  $A + B \rightarrow C$  type reaction-diffusion process. *Phys Rev A* 1988;38:3151–4.
- [66] Koo YEL, Kopelman R. Space- and time-resolved diffusion-limited binary reaction kinetics in capillaries: experimental observation of segregation, anomalous exponents, and depletion zone. *J Stat Phys* 1991;65:893–918.
- [67] Taitelbaum H, Havlin S, Kiefer JE, Trus B, Weiss GH. Some properties of the  $A + B \rightarrow C$  reaction-diffusion system with initially separated components. *J Stat Phys* 1991;65:873–91.
- [68] Taitelbaum H, Koo YEL, Havlin S, Kopelman R, Weiss GH. Exotic behavior of the reaction front in the  $A + B \rightarrow C$  reaction-diffusion system. *Phys Rev A* 1992;46:2151–4.
- [69] Ben-Naim E, Redner S. Inhomogeneous two-species annihilation in the steady state. *J Phys A: Math Gen* 1992;25:L575–83.
- [70] Araujo M, Larralde H, Havlin S, Stanley HE. Scaling anomalies in reaction front dynamics of confined systems. *Phys Rev Lett* 1993;71:3592.
- [71] Barkema GT, Howard MJ, Cardy JL. Reaction-diffusion front for  $A + B \rightarrow \emptyset$  in one dimension. *Phys Rev E* 1996;53:R2017(R).
- [72] Koza Z, Taitelbaum H. Motion of the reaction front in the  $A + B \rightarrow C$  reaction-diffusion system. *Phys Rev E* 1996;54:R1040(R).
- [73] Taitelbaum H, Koza Z. Anomalous kinetics of reaction-diffusion fronts. *Philos Mag B* 1998;77:1389–400.
- [74] Park SH, Parus SP, Kopelman R, Taitelbaum H. Gel-free experiments of reaction-diffusion front kinetics. *Phys Rev E* 2001;64:055102(R).
- [75] Rongy L, Trevelyan PMJ, De Wit A. Dynamics of  $A + B \rightarrow C$  reaction fronts in the presence of buoyancy-driven convection. *Phys Rev Lett* 2008;101:084503.
- [76] Rongy L, Trevelyan PMJ, De Wit A. Influence of buoyancy-driven convection on the dynamics of  $A + B \rightarrow C$  reaction fronts in horizontal solution layers. *Chem Eng Sci* 2010;65:2382–91.
- [77] Eckert K, Rongy L, De Wit A.  $A + B \rightarrow C$  reaction fronts in Hele-Shaw cells under modulated gravitational acceleration. *Phys Chem Chem Phys* 2012;14:7337–45.
- [78] Tiani R, Rongy L. Influence of Marangoni flows on the dynamics of isothermal  $A + B \rightarrow C$  reaction fronts. *J Chem Phys* 2016;145:124701.